Supplement of Atmos. Chem. Phys., 21, 12261–12272, 2021
https://doi.org/10.5194/acp-21-12261-2021-supplement

Atmospheric Chemistry and Physics Open Access

Supplement of

Deciphering organization of GOES-16 green cumulus through the empirical orthogonal function (EOF) lens

Tom Dror et al.

Correspondence to: Ilan Koren (ilan.koren@weizmann.ac.il)

Contents of this file

1. Text S1 to S2
2. Movie caption
3. Figures S1 to S7

Additional Supporting Information (Files uploaded separately)

1. Movie S1 (https://doi.org/10.34933/wis.000007)

General comments

This Supporting Information (SI) contains detailed explanations regarding (i) the gamma correction applied to the reflectance images prior to the analyses, and (ii) the calculation and derivation of spatio-temporal characteristics of the gravity waves (GW) and the cloud streets (Text S1). An explanation regarding the identification of the different types of clouds exhibited in the region of interest (ROI) (Text S2). It also presents the caption for the video (Movie S1; uploaded separately) showing the diurnal evolution of the cloud field. Additionally, it includes Figs. S1,S2, showing the diurnal evolution of cloud properties, the topography of the examined ROI (Fig. S3), and a figure showing the early–morning clouds (Fig. S4). Finally, figures showing EOF3–EOF8 (Fig. S5), EOF9–EOF14 (Fig. S6) and EOF15–EOF20 (Fig. S7) are also included.

Text S1.

Gamma correction. The reflectance images obtained from GOES–16 ABI's "Red" band looked somewhat dark, since the values were in linear units. In such cases, it is a common practice to adjust and brighten the images by applying a simple gamma correction as follows: $I_{out} = AI_{in}^{\gamma}$, where I_{in} is the darker input image, $\gamma = 0.5$, $A = 1$, and I_{out} is the adjusted image (corrected reflectance).

Spatio-temporal characteristics of GW and cloud streets. The GW wavelength ℓ is estimated using EOF5 and EOF6 as follows:

$$\ell = \frac{\lambda_5 \ell_5 + \lambda_6 \ell_6}{\lambda_5 + \lambda_6}$$

where $\lambda_{5,6}$ are the eigenvalues associated with EOF modes 5 and 6, respectively, and ℓ_j ($j = 5, 6$) denotes the euclidean distance between two consecutive wave fronts as captured by EOF5 and EOF6 and marked by dashed lines in Fig. S5-(c,d).

The cloud street's aspect ratio (AR) is defined as the streets wavelength divided by the convective boundary layer (CBL) depth following Young et al. (2002). To estimate the street's AR we calculate their mean wavelength from Fig. 6-(d) in the Main Text for a CBL depth of 1 km. The latter is estimated from the range of green cumulus (Cu) cloud top height (CTH) during the eight hours of the inspected time–span, since shallow Cu are known to be capped by the inversion that defines the CBL depth (Zhang and Klein, 2013).

Text S2.

Cloud Identification. The region of interest (ROI) analysed in the paper along the eight hours of Aug 22, 2018, consists of a few types of clouds. The predominant cloud type is green Cu, which consists of shallow, small, liquid clouds, with tops ranging between $800 - 1800\,m$ (see Figs. S1,S2). However, other types of clouds are present in the ROI throughout the day. Using cloud properties such as cloud top phase (Fig. S1) and CTH (Fig. S2), and the topography (Fig. S3), we determine the other types of clouds. We identify deeper, warm orographic clouds with tops $\sim$3000 m, during the noon and afternoon, at the north-eastern

part of the domain, above the south edge of the Appalachians (see Fig. S3). Also, Cirrus clouds with ice tops that reach as high as $\sim$12000m (above the green Cu) prevail in the morning in the northern-central part of the ROI and move southward along the day. Norther to Florida, shallow liquid clouds, with tops ranging between a few hundreds meters and up to $\sim$2500m are present in the early-morning and dissipate around 11:30 eastern standard time (EST) (see movie S1, and Fig. S4). Finally, deep clouds with cold, high tops, that appear at the morning-time over Northern Florida evolve throughout the day (see movie S1 and Figs. S1,S2,S4). Note that even though the cirrus clouds cover substantial parts of the ROI throughout many hours of the inspected time frame (see Figs. S1,S2), they are almost transparent in the visible channel on which we preform the analyses, thus we consider the green Cu as the leading mode throughout the time frame of this study, and we focus on their evolution in the main text.

Movie S1–Caption.
Diurnal evolution (10:47–18:47 EST) of the cloud field demonstrated by the corrected reflectance field as obtained from GOES–16 ABI's "Red" visible band (band 2; 0.64μm).

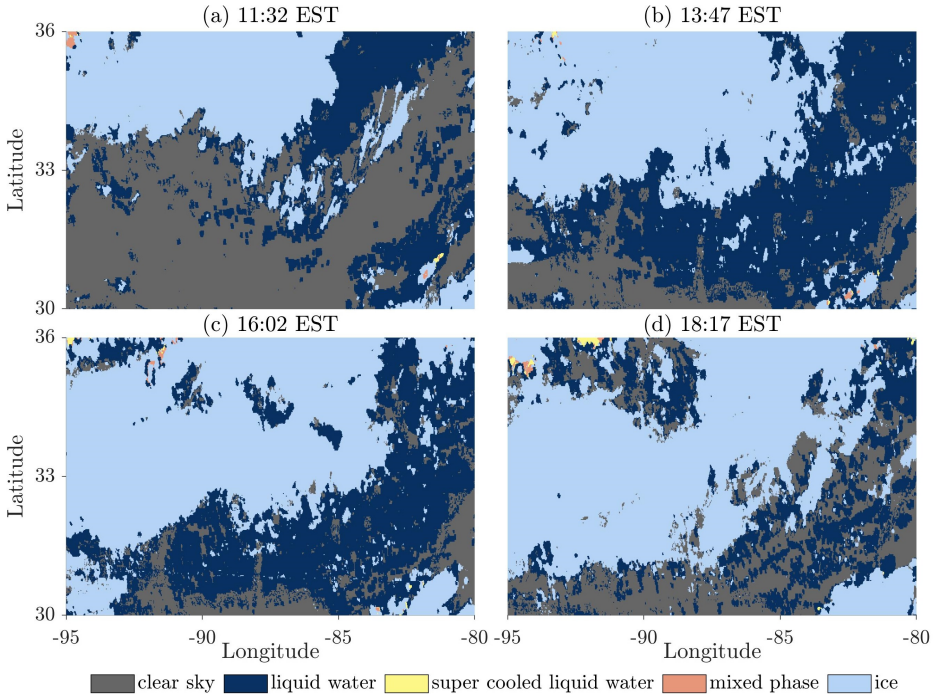

Figure S1. Cloud top phase of the diurnal cloud field evolution as obtained from GOES–16 ABI's L2 cloud top phase product (2km resolution). Snapshots taken at 11:32 **(a)**, 13:47 **(b)**, 16:02 **(c)**, and 18:17 **(d)** EST.

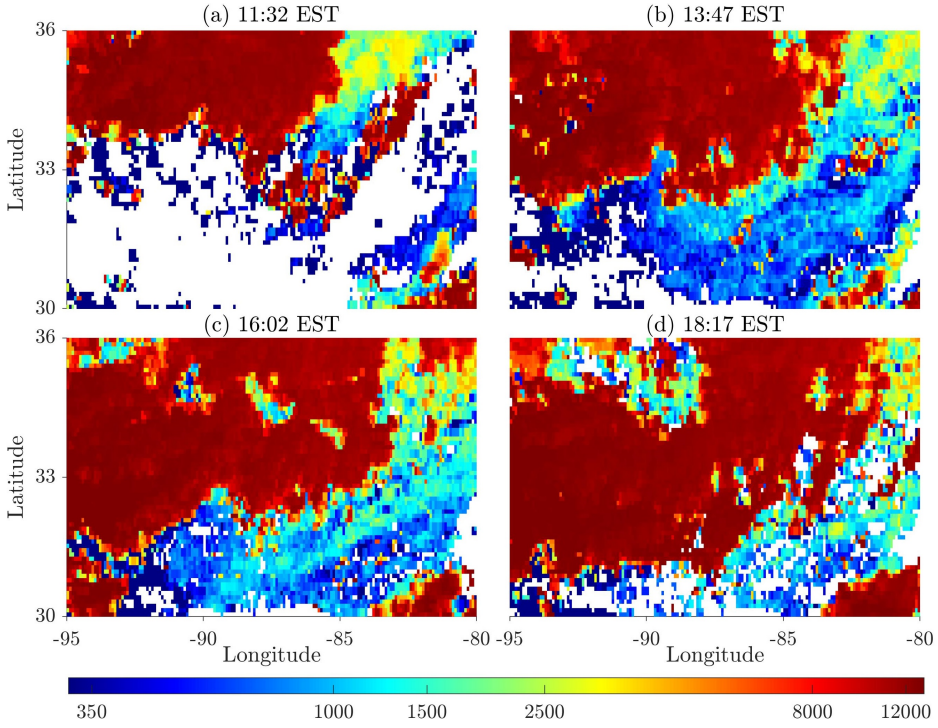

Figure S2. Same as Fig. S1 but for cloud top height (m) as obtained from GOES–16 ABI's L2 cloud top height product ($10\,km$ resolution).

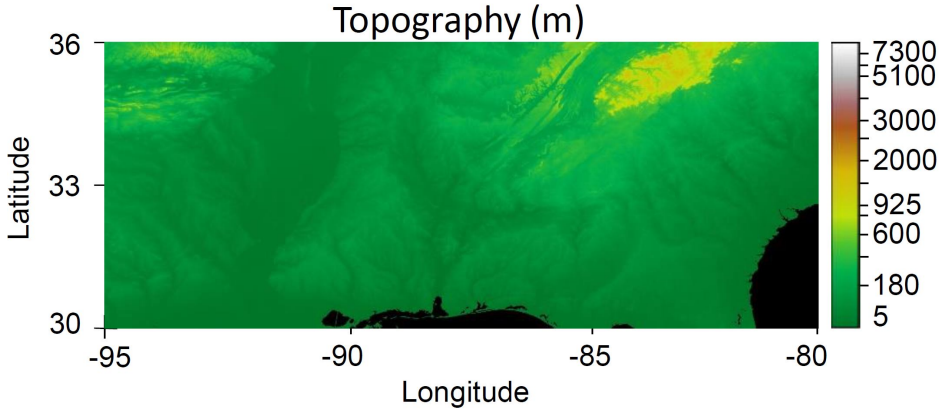

Figure S3. Topography (m) from the Shuttle Radar Topography Mission (SRTM) data product (SRTMGL1), obtained from Worldview.

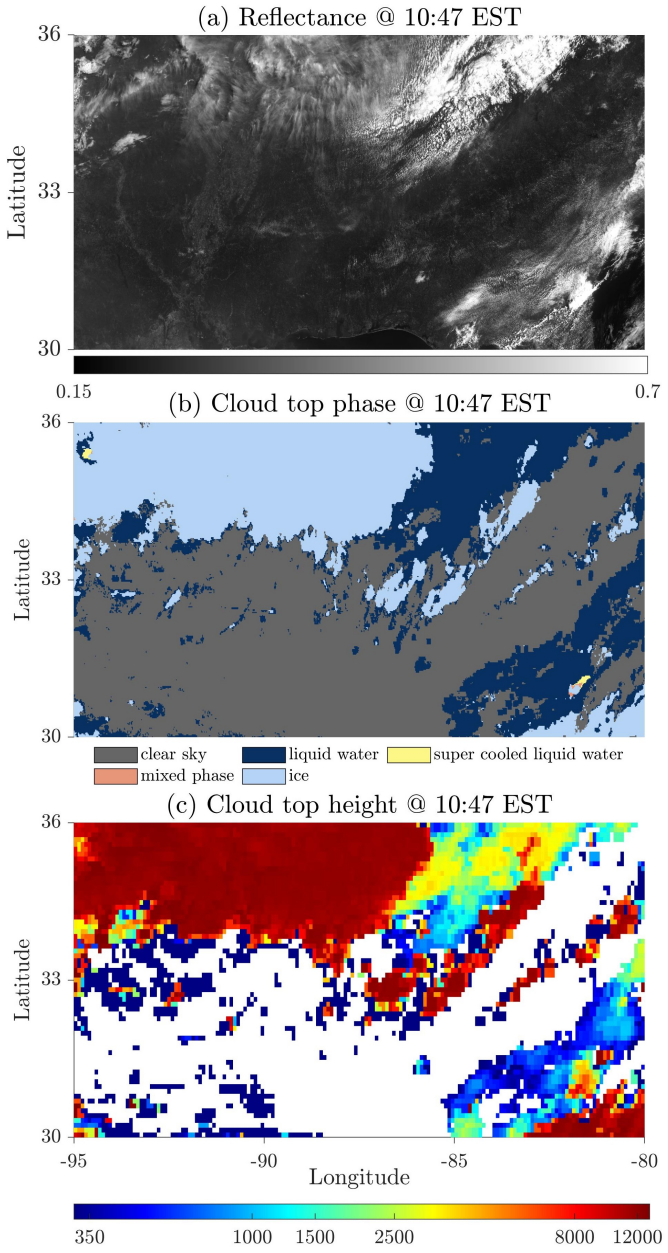

Figure S4. Corrected reflectance **(a)**, clout top phase **(b)**, and cloud top height (m) **(c)** of the ROI at 10:47 EST.

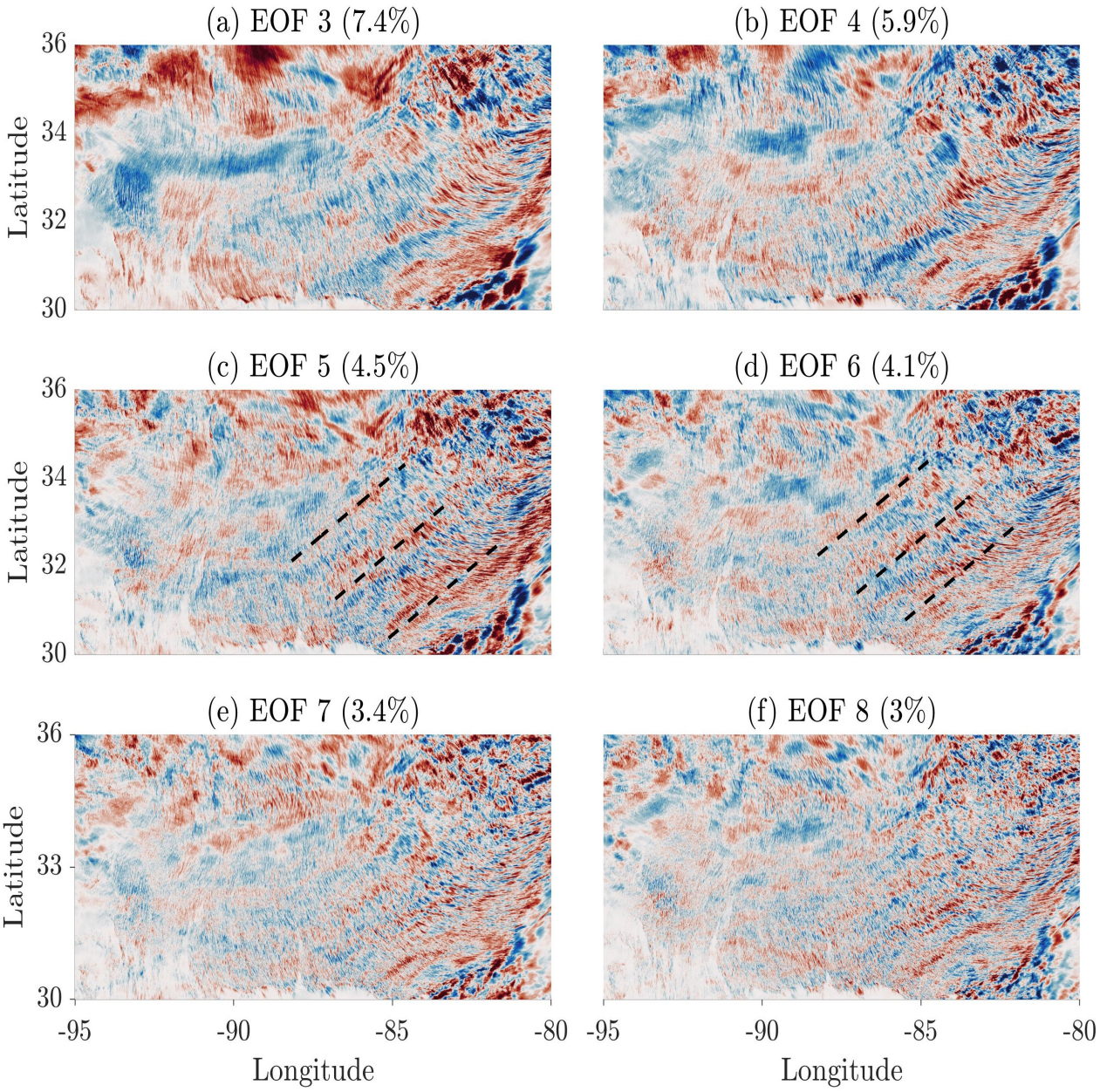

Figure S5. EOF modes 3–8, units are arbitrary (the variance explained by each of the modes is noted at the title of each panel). Dashed lines in **(c)** and **(d)** mark the axis of gravity waves.

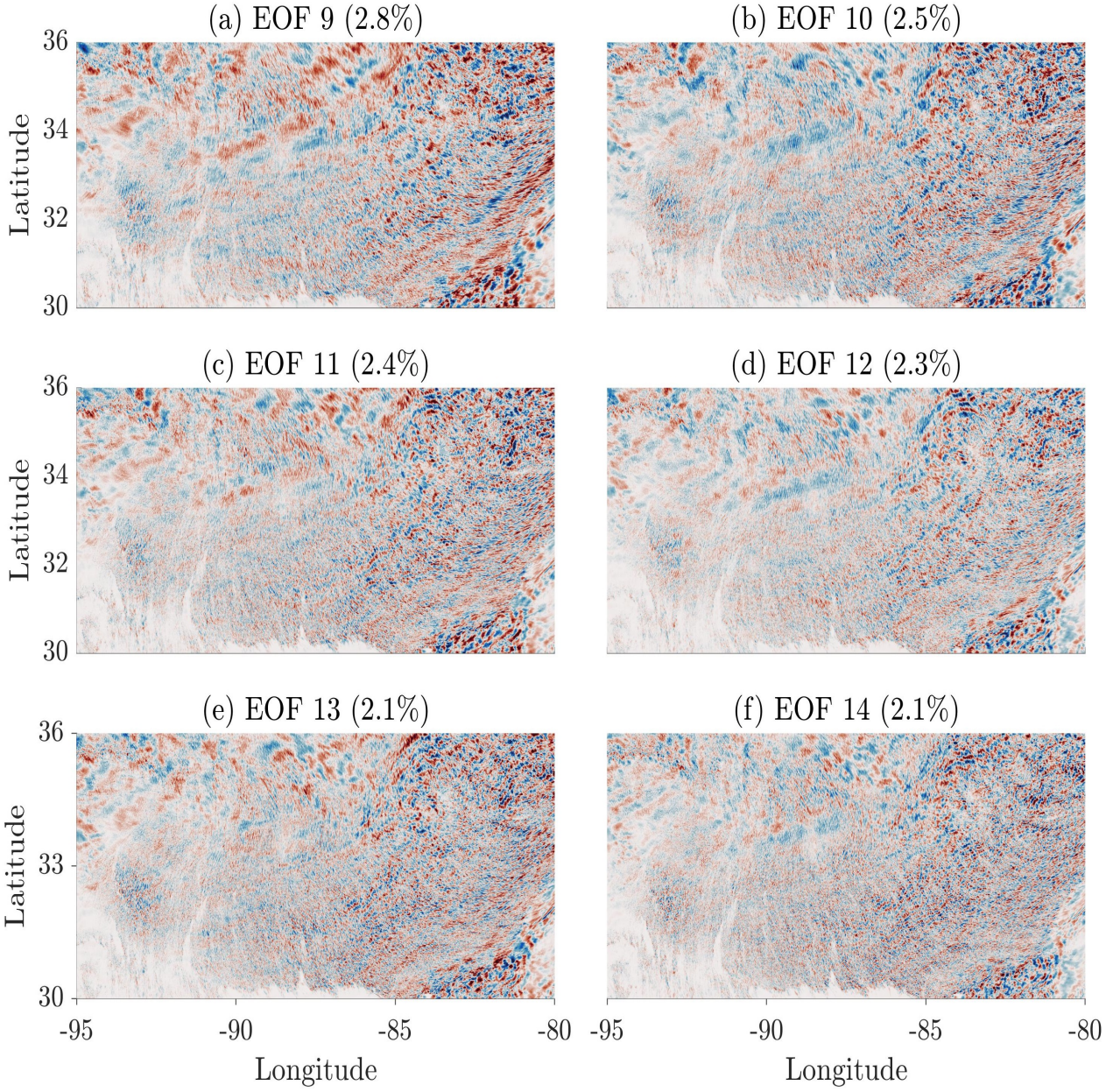

Figure S6. Same as Fig. S5 but for EOF modes 9–14.

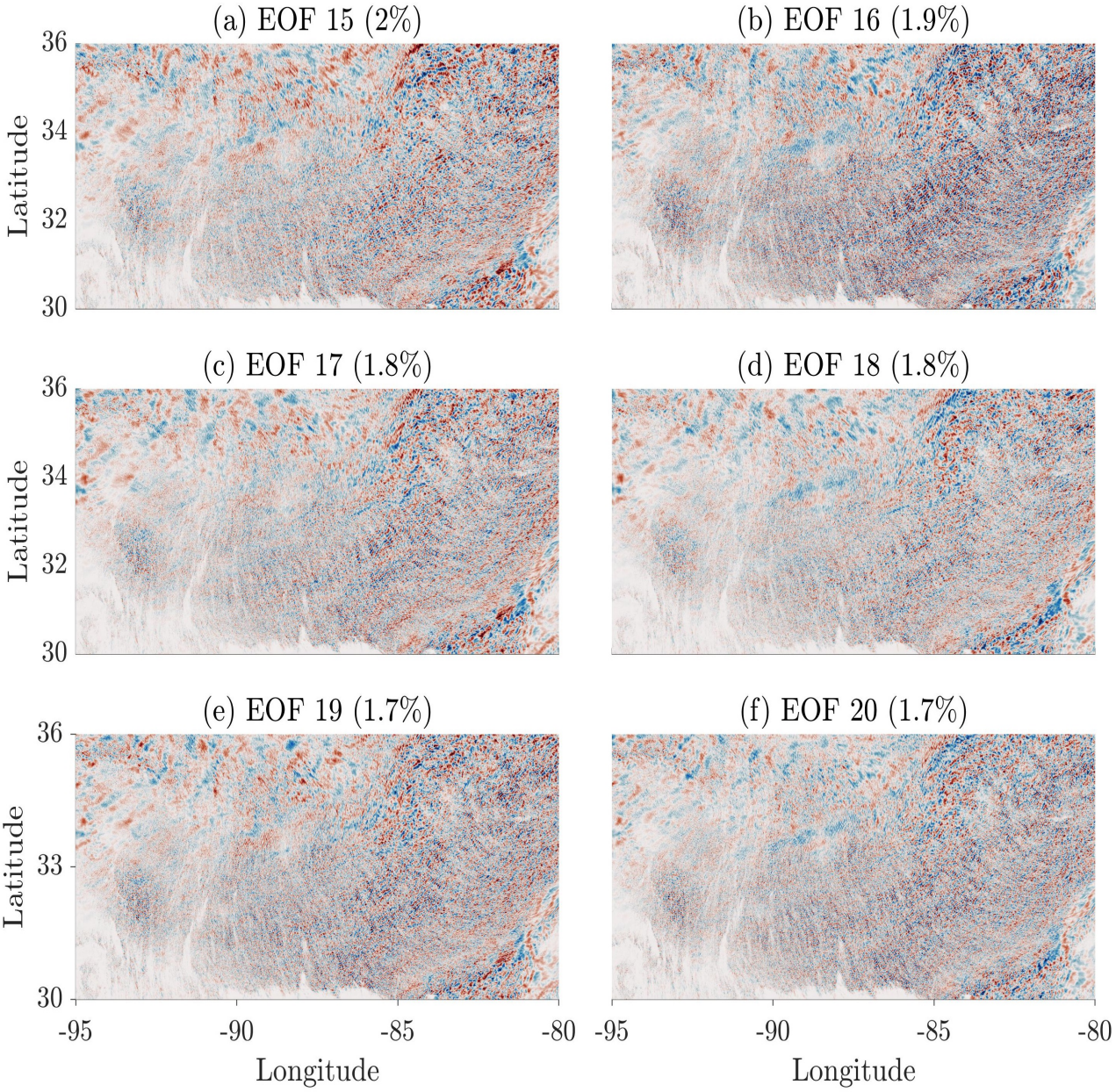

Figure S7. Same as Fig. S5 but for EOF modes 15–20.

References

Young, G. S., Kristovich, D. A., Hjelmfelt, M. R., and Foster, R. C.: Rolls, streets, waves, and more: A review of quasi-two-dimensional structures in the atmospheric boundary layer, Bulletin of the American Meteorological Society, 83, 997–1002, 2002.

Zhang, Y. and Klein, S. A.: Factors Controlling the Vertical Extent of Fair-Weather Shallow Cumulus Clouds over Land: Investigation of Diurnal-Cycle Observations Collected at the ARM Southern Great Plains Site, Journal of the Atmospheric Sciences, 70, 1297–1315, https://doi.org/10.1175/JAS-D-12-0131.1, 2013.